



OPEN

Effect of TX-100 pretreatment on carbon paste electrode for selective sensing of dopamine in presence of paracetamol

J. K. Shashi Kumara¹, B. E. Kumara Swamy^{1✉}, G. K. Jayaprakash², S. C. Sharma^{3,4✉}, Roberto Flores.-Moreno⁵, Kaustubha Mohanty⁶ & S. A. Hariprasad⁷

Dopamine (DA) is one of the chief neurotransmitters present in the central nervous system of mammals. Therefore detection of DA in presence of various analytes like paracetamol has great importance. In the current work, we are proposing that Triton X-100 (TX-100) pretreated carbon paste electrode (CPE) can be useful to detect the DA selectively in presence of PA. After the pretreatment CPE can detect DA in presence of PA effectively. Cyclic voltammetry was employed to observe the amplified electron transfer reaction between the modified CPE and DA. To understand electron transfer regioselectivity at the TX-100 pretreated CPE, a dual descriptor was used. The prepared electrode showed satisfactory stability when kept under ambient conditions. The proposed approach also showed excellent analytical applicability to identify DA and PA in commercial formulations. The scope of the work is limited to detecting DA in presence of PA. We will consider the other interferes for future works.

Now-day researchers are more concentrating on carbon paste electrodes (CPEs) to utilize them as working electrodes in electrochemical sensors applications. CPEs offer several appealing properties, including surface repeatability, stability, and renewability, making them appealing substances for working electrodes^{1–3}. Due to their inexpensive cost relative to other materials, CPEs are becoming more widely used in areas such as pharmaceutical, biological, and environmental analysis^{4,5}.

Physical or chemical modifications can improve CPE's sensing properties like selectivity, adsorption capacity, and sensitivity^{6,7}. The goal of modifying a CPE matrix is to create an efficient electrode with sensing properties that will be useful for users. In general, after modifications, electrocatalytic activities at the CPE interface will improve, which may be due to the increased surface area which in turn gives better current sensitivity for electron transfer reactions. CPE can be chemically modified using conductive substrates modified with electroactive thin films, monolayers, or thick coatings^{8,9}.

The electrochemical modifications may include the use of different types of surfactants to modify the CPE. Clay minerals treated with surfactants have excellent sorption capabilities for both organic and inorganic substances in aqueous solutions^{10,11}. In terms of electrode modification, T-octylphenoxypolyethoxyethanol (Triton X-100 (TX100)) is one of the best nonionic surfactants^{12–16}. The properties of hybrid materials (carbon paste + TX-100) are highly promising. TX-100 modified carbon hybrid materials are previously reported to use as electrodes. TX-100 adsorbed electrode alters the electrode–electrolyte interface, making it easier to create poly (m-toluidine) films with higher current densities¹⁶. TX-100 modified CPE was prepared by surface immobilization technique by B.N. Chandrashekar et al. and this method exhibit good sensitivity, but TX-100 pretreatment is more applicable than this method¹⁷. According to the literature, modification of electrodes using

¹Department of P.G. Studies and Research in Industrial Chemistry, JnanaSahyadri, Kuvempu University, Shankaraghatta, Shivamogga, Karnataka 577451, India. ²Department of Chemistry, Nitte Meenakshi Institute of Technology, Bangalore, Karnataka 560064, India. ³National Assessment and Accreditation Council (Work Carried Out As Honorary Professor), Jain University, Bangalore, Karnataka 560 069, India. ⁴School of Energy Science and Engineering, Indian Institute of Technology Guwahati, Guwahati 781039, India. ⁵Departamento de Química, Centro Universitario de Ciencias Exactas e Ingenierías, Universidad Guadalajara, Blvd. Marcelino García Barragán N 1421, C.P. 44430 Guadalajara, Jal., Mexico. ⁶Department of Chemical Engineering, Indian Institute of Technology Guwahati, Guwahati 781039, India. ⁷Jain University, Bangalore, Karnataka 560 069, India. ✉email: bek@kuvempu.ac.in; scsharma.bangalore@gmail.com

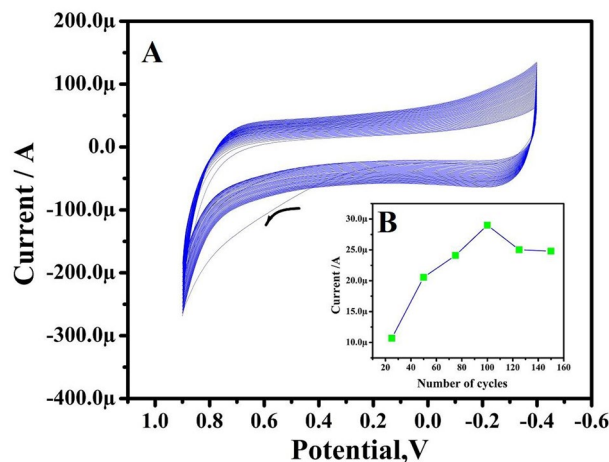


Figure 1. (A) CVs for electrodeposition of TX-100 on a BCPE in 0.1 M NaOH by 100 cycles. Sweep rate: 1 Vs^{-1} . (B) The graph of anodic peak current versus several cycles for potassium ferrocyanide at a sweep rate of 50 mV/s.

TX-100 has several works but the pre-treatment method good one for analysis of biomolecules proved by the present work^{18,19}.

The modifications of electrodes can be done by methods like mechanical grinding, self-assembled layers, covalently bonded electrolyzers, surfactant immobilization, etc. The electrochemical pre-treatment process increases the electron transfer compared to others. To use carbon surface effectively one must take care of the degree of activation²⁰. The modification of CPEs is achieved simply by pre-treatment of TX-100 modifier with the carbon paste which is enhancing the sensitivity and selectivity of the electrochemical analysis technique.

Because of its simplicity, sensitivity, efficiency, and low cost, electrochemical pretreatment was chosen for this study. Pretreatment is considered environmentally benign since it uses less dangerous chemicals than other time-consuming and sophisticated modification materials. The electrochemical pretreatment procedure results in transducers that produce signals that are undistorted, well-defined, and repeatable. By creating charge-carrying functional groups, the pretreatment of the CPE enhances the selectivity and sensitivity of the sensors for detecting selected electroactive components. In the present work, we study the effect of TX-100 pretreatment on CPE, and it is used in applications for DA and PA sensors with performing the detection of DA in the presence of PA because the usage of PA protects dopaminergic neurons against oxidative stress damage produced by acute exposure to increased amounts of DA, according to *in vitro* studies²¹ and it shows outstanding stability, sensitivity, and selectivity for biomedical applications.

Experimental section

Reagents and chemicals. Paracetamol (PA) was obtained from Merck, sodium hydroxide (NaOH), and dopamine hydrochlorides (DA) from nice chemicals. The graphite powder (LobaChemie), Silicone oil and TX-100 are obtained from Himedia.

Apparatus. The TX-100 atomic model has created with Sinapsis software (Version: Sinapsis.XIII Weblink: <http://sinapsis.sourceforge.net> Access date: accessed July 20, 2020)²². The experiments were done using the potentiostat model CHI-660c (CH Instrument-660 electrochemical workstation) and the generated data was transferred to origin 6.1. Bare CPE (BCPE), NaOH pretreated modified CPE (NaOH-PT-MCPE), and TX-100 pretreated modified CPE (TX-100PT-MCPE) are used as working electrodes, saturated calomel as the reference electrode, and a platinum electrode as a counter electrode.

Preparation of BCPE. The BCPE was prepared by hand mixing 70% graphite powder with 30% silicon oil in an agate mortar for approximately 30 min to produce a homogenous carbon paste. The paste was packed into the homemade cavity of a Teflon tube and polished on a paper napkin to obtain a uniform surface.

Pretreatment of CPE with TX-100. The pretreatment process was carried out using cyclic voltammetry (CV), potential cycles were between -0.4 and 0.9 V at a scan rate (v) of 1 V/s for 100 cycles as depicted in Fig. 1A. With an increase in the cycle number voltammogram, currents decreased gradually which indicates that during the pretreatment process TX-100 is adsorbing on the electrode surface. To eliminate contaminants electrode was dipped in deionized water. The electrochemical response of TX-100PT-MCPE with different cycles is measured by using potassium ferrocyanide, $\text{K}_4(\text{Fe}(\text{CN})_6)$ at a sweep rate of 50 mV/s is depicted in Fig. 1B. TX-100PT-MCPE prepared by 100 cycles showed better sensing capability hence it is considered for further analysis.

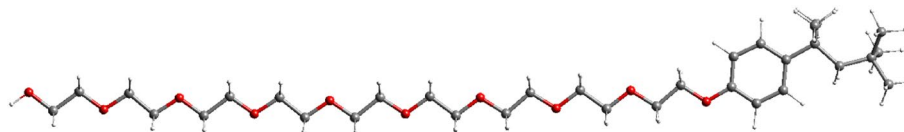


Figure 2. Atomistic model of Triton X-100 (H = white, C = grey, and O = red).

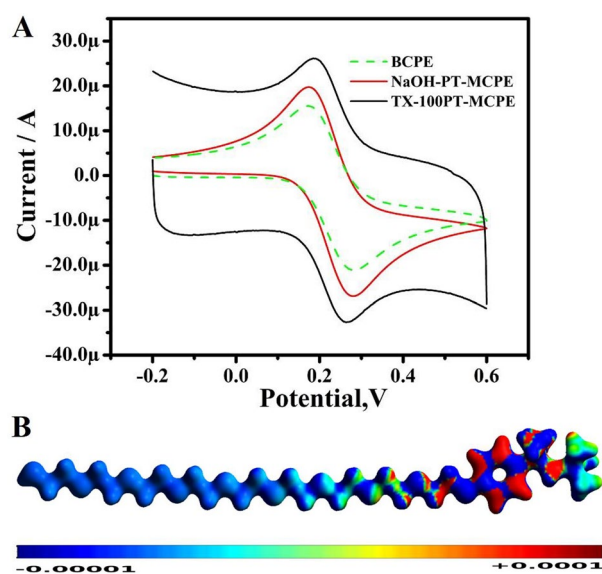


Figure 3. (A) CVs of 1 mM potassium ferrocyanide in 1 M KCl solution at a speed rate of 50 mV/s. (B) Dual descriptor result of TX-100 [ISO = 0.07, grid = 0.3].

Electrodes	I_{pa} (A)	ΔE (V) [at $v = 0.05$ V]	Area (cm^2)
BCPE	2.12×10^{-05}	0.110	0.0321
Pretreated NaOH MCPE	2.70×10^{-05}	0.103	0.0372
PTTMCE	3.26×10^{-05}	0.050	0.0412

Table 1. The electrochemical performance of the electrodes.

Computational analysis. The TX-100 atomic model was created with Sinopsis software²² as shown in Fig. 2 and geometry optimization was done with deMon2k software²³ using PBE exchange - correlation functions^{24,25} and TZVP basis sets²⁶, employing density functional theory (DFT) as described in our previous articles. Sinopsis software was used to plot the dual descriptor results.

Results and discussion

The PTTMCE electrochemical response towards potassium ferrocyanide. The cyclic voltammetric (CV) response of $K_4(Fe(CN)_6)$ at TX-100-PTMCE is shown in Fig. 3A. The BCPEs had poor peak current and high redox peak potential differences, but the MCPEs had much-improved redox peak current signals and smaller redox peak potential discrepancies. Randle's Sevcik's equation²⁷ was used to calculate the total active surface area. The active surface area for electrodes (BCPE, NaOH-PT-MCPE, and TX-100PT-MCPE) is shown in Table 1.

The heterogeneous rate constant (k^0) values for $K_4(Fe(CN)_6)$ are calculated from the ΔE_p values (> 10 mV) using Eq. (1). The k^0 values are listed in Table 2.

$$\Delta E_p = 201.39 \log(v/k^0) - 301.78 \quad (1)$$

TX-100 redox sites are found using ADPT-based dual descriptor calculations. The dual descriptors or dual Fukui functions are obtained using Fukui functions. Fukui functions can be defined according to Eq. (2)²⁶. Previously we have used the Fukui functions to analyze surfactants^{28,29}.

v/mV/s	$\Delta E_p/mV$			$k^s(s^{-1})$		
	BCPE	Pretreated NaOH MCPE	PTT MCPE	BCPE	Pretreated NaOH MCPE	PTT MCPE
50	110	103	50	0.895798	0.488696	0.451108
100	131	130	82	0.709635	0.717796	1.242637
150	141	140	87	0.949449	0.960367	1.760387
200	153	150	97	1.103633	1.142144	2.093592
250	159	158	104	1.288076	1.302888	2.415703

Table 2. The rate constant values for potassium ferrocyanide at different electrodes.

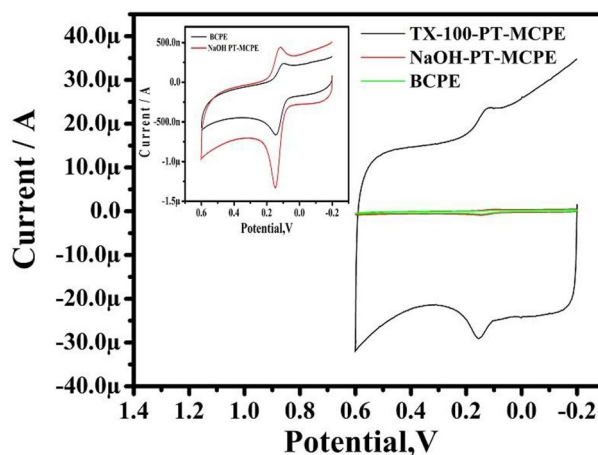


Figure 4. CVs for 10 μM DA in 0.2 M PBS solution of pH 7.4 at pretreated NaOH and TX-100-PT-MCPE at the sweep rate of 100 mV/s. Inset: compares the BCPE and NaOH pretreatment.

$$f^{\pm}(r) \equiv \lim_{\Delta N \rightarrow 0^{\pm}} \frac{\rho_{N+\Delta N}(r) - \rho_N(r)}{\Delta N} \quad (2)$$

where N is the number of electrons in the system, $\rho(r)$ is the electron density, + and - signs correspond to the addition or removal of electrons, respectively. The dual descriptor (f_D) is plotted using Eq. (3).

$$f_D = f^+ - f^- \quad (3)$$

The dual descriptor charts for TX-100 are shown in Fig. 3B²². The blue colour regions in our dual descriptor maps indicate TX-100 oxidation sites, whereas the red colour regions represent TX-100 reduction sites. TX-100 is oxidized via the tail due to the presence of oxygen atoms with lone pair electrons, and it is reduced via the head phenyl ring.

The electrochemical response for DA at PTTMCPE. The voltammetric response of DA (10 μM) at the BCPE, NaOH-PTMCPE, and TX-100PT-MCPE was displayed in Fig. 4. The peak potential difference (ΔE_p) was 58 mV at BCPE. However, ΔE_p values are 28 mV and 25 mV for NaOH-PT-MCPE and TX-100-PTMCPE respectively. This indicates that pretreated electrodes are good for sensing applications.

Electrochemical investigation of DA with the different parameters at TX-100-PT-MCPE. As shown in Fig. 5A, the effect of change in the v for 10 μM DA in 0.2 M PBS was studied by CV at TX-100PT-MCPE. The TX-100PT-MCPE demonstrates that as the v increases the redox peak current steadily increases. The plot of anodic peak current (I_{pa}) vs v verifies the type of electrode process (Inset of Fig. 5B). The correlation coefficient was originally set at $R^2 = 0.9997$, however, Fig. 5C depicts a plot of $\log I_{pa}$ vs $\log v$ with 0.8362 slopes. Therefore, the mass transfer process is adsorption controlled³⁰.

Figure 6A displays the CV response of DA at TX-100-PT-MCPE at different concentrations of 10–60 μM using 0.2 M PBS (pH 7.4) with a v 100 mV/s. With a rise in concentration, the corresponding anodic peak current (I_{pa}) of DA enhances. Figure 6B shows the curve of I_{pa} vs DA concentration. It has high linearity with regression equations are $I_{pa}(\mu A) = 42 (\mu M) + 0.105$ ($R^2 = 0.9981$) and the limit of detection (LOD) and limit of quantification (LOQ) are calculated according to Eqs. (4, 5)³⁰. Where S is the standard deviation and M is the slope obtained from the calibration plot:

$$LOD = 3S/M \quad (4)$$

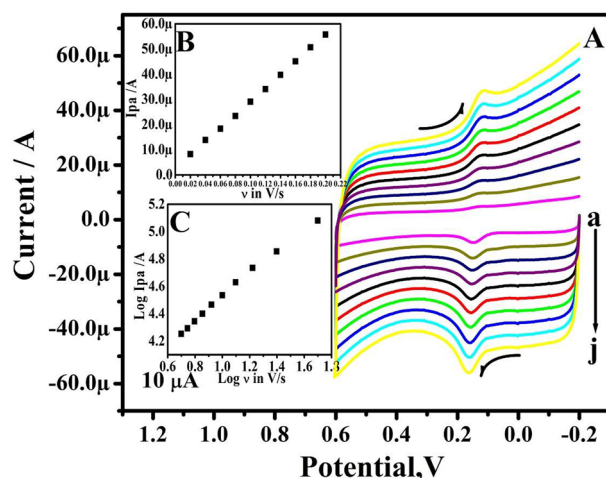


Figure 5. (A) CVs of 10 μM DA in 0.2 M PBS solution of pH 7.4 at TX-100-PT-MCPE at different sweep rates. (a–j; 20–200 mV/s). (B) Graph of peak current versus sweep rate. (C) Graph of the log of peak current versus the log of sweep rate.

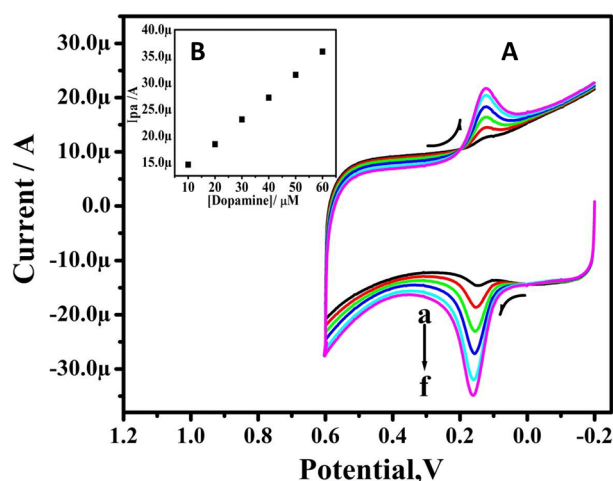


Figure 6. (A) CVs of 10 μM DA in 0.2 M PBS solution of pH 7.4 at TX-100-PT-MCPE at a sweep rate of 50 mV/s with different concentrations (a–f: 10–60 μM). (B) Graph of anodic peak current versus concentration of DA.

$$\text{LOQ} = 10\text{S/M} \quad (5)$$

The comparative analytical performance electrode for DA was presented in Table 3^{31–47} and LOQ was found to be 4.08 μM .

The CVs for DA obtained by the TX-100-PT-MCPE at v of 100 mV/s in PBS of various pH from 6.2 to 7.8 for DA are shown in Fig. 7A. The I_{pa} of DA changed to a less positive potential as the pH increased. A graph of E_{pa} vs different pH levels was used to create the potential diagram (Fig. 7B). With a slope of 55 mV/pH, the obtained graphs exhibit acceptable linearity with regression equations are E_{pDA} (mV) = $-55 \text{ pH} + 56$ ($R^2 = 0.9989$). The calculated slope is extremely near to the Nernstian value of 59 mV, as shown in the graphs. Therefore, an equal number of protons and electrons are transferred in the reactions (Fig. 7C).

Electrochemical investigation of PA with different parameters at TX-100PT-MCPE. A CV profile of 10 μM PA at BCPE and TX-100PT-MCPE in 0.2 M PBS is shown in Fig. 8 (pH 7.4). The TX-100PT-MCPE shows an increase in redox I_{pa} and a small shift in potential, but the BCPE, PA shows less current and more widespread peaks. Our findings show that following the change, the electrode performs well and lowers ΔE while increasing I_{pa} . These findings show that the proposed sensor has a catalytic effect on PA analysis.

At TX-100-PT-MCPE, the effect of v on the CV performance of the PA was investigated in PBS (pH 7.4). I_{pa} increased with a slight positive shift in the peak potential displayed in Fig. 9A increased in the region of

Sl. no.	Electrodes	Linear range (μM)	LOD (μM)	Method	References
01	Au/Gr-Au	0.03–30	30	SW	31
02	Pt–Au hybrid	103–165	24	CV	32
03	CTAB/CPE	0–130	11.0	DPV	33
04	Fc-MCPE	120–11,000	9.4	CV	34
05	Poly (Sudan III)/MCPE	10–60	9.3	CV	35
06	SWCNT/GCE	–	7.0	DPV	36
07	Metallothioneins self-assembled gold electrode	0.08–0.2	6.0	CV	37
08	LDH/CILE	10–1100	5.0	DPV	38
09	Ag-reduced GO/GCE	10–800	5.4	LSV	39
10	Poly-VA/MWCNT/GCE	5–120	4.5	CV	40
11	Ag/Ag ₂ S-CNT-Nafion	250–2000	4.7	DPV	41
12	BPVCM-e/MWCNT/GCE	5–5000	2.25	CV	42
13	Poly (amido black) MCPE	10–60	2.03	CV	43
14	CTAB-GO/MWNT	5.0–500	1.5	DPV	44
15	TX-100-PT-MCPE	10–60	1.22	CV	Present work
16	SiTi/AuNP/CPE	20–180	0.57	CV	45
17	Ni-Zr/MSN/GCE	0.3–100	0.13	CV	46
18	PSi NPs modified GCE	0.5–333.3	0.032	CV	47

Table 3. Comparative analytical performance electrode for DA.

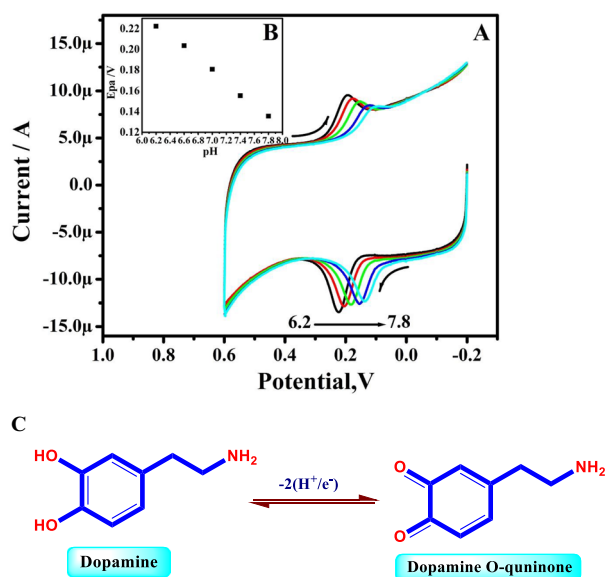


Figure 7. (A) CVs of 10 μM DA for different pH (6.2–7.8 pH) at TX-100-PT-MCPE. (B) Graph of E_{pA} versus different pH. (C) Redox mechanism dopamine.

20–200 mV/s. In Fig. 9B,C, the current intensity changes in terms of sweep rates are shown in a graph with good linearity. The findings show that the oxidation–reduction process of PA is influenced by adsorption.

PA CVs at TX-100-PT-MCPE at various concentrations are depicted in Fig. 10A. PA's I_{pa} hikes with an increase in concentration shown in Fig. 10B. The linearity of the I_{pa} vs. PA concentration was found high linearity with regression equations are $I_{pa}(\mu\text{A}) = 01 (\mu\text{M}) + 0.15$ ($R^2 = 0.99979$) and the limit of detection (LOD) and limit of quantification (LOQ) are calculated according to Eqs. (4, 5) and are found to be 5.031 μM and 16.77 μM respectively.

The CVs profile for PA, at TX-100-PT-MCPE in 0.2 M PBS range 6.2–7.8 is portrayed in Fig. 11A. The E_{pa} was moved negative with an increase in pH values. Figure 11B portrayed the linear establishment between E_{pDA} and pH and provide a slope of 57 mV for PA with regression equations are $E_{pDA} (\text{mV}) = -57 \text{ pH} + 58$ ($R^2 = 0.9997$). The resulting slope is close to the Nernstian value. Therefore, an equal number of protons and electrons are transferred in the reactions (Fig. 11C).

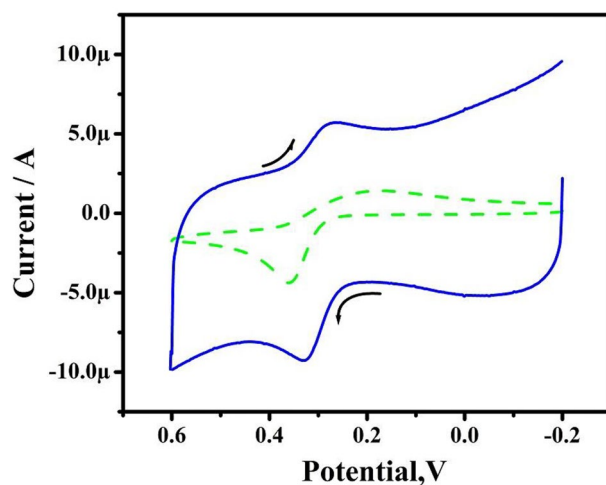


Figure 8. CVs of 10 μM PA in 0.2 M PBS solution of pH 7.4 at BCPE and TX-100-PT-MCPE at the sweep rate of 100 mV/s.

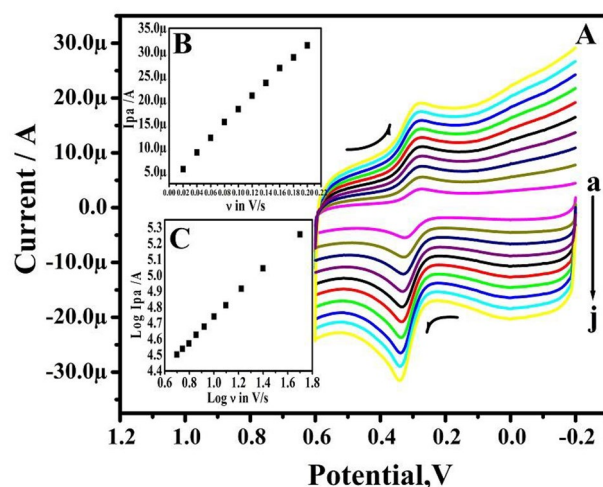


Figure 9. (A) Cyclic voltammograms of 10 μM PA in 0.2 M PBS solution of pH 7.4 at TX-100-PT-MCPE at different sweep rates. (a–j; 20–200 mV/s). (B) Graph of peak current versus sweep rate. (C) Graph of the log of peak current versus the log of sweep rate.

Selectivity and reproducibility study for TX-100-PT-MCPE. Figure 12A displays the CV responses of 10 μM of DA and 10 μM PA in 0.2 M PBS of both BCPE and TX-100PT-MCPE. The BCPE showed short current signals with poor selectivity indicating that electrode is not selective for simultaneous detection of DA and PA. But after TX-100 pretreatment current signals are enhanced and selectivity was improved (oxidation potential of DA and PA are separated). Therefore, TX-100PT-MCPE can effectively be used to detect DA in presence of PA. The fabrication reproducibility was checked by successively scanning 50 cycles depicted in Fig. 12B. The I_p signals retained approximately 90.6% of the original value. The experimental results indicated that the TX-100PT-MCPE possesses a long service life.

Interference study. Figure 13A displays the DPVs of DA at 5–40 μM concentration in presence of 5 μM PA. As a result, the I_{pa} of DA increases with an increase in DA concentration, and the I_{pa} of PA remains constant. The obtained results are good as shown in the graph of I_{pa} versus the concentration of DA (Fig. 13B). This indicates that TX-100-PT-MCPE can selectively sense DA in presence of PA.

Figure 14A demonstrates raising the concentration of PA from 5 to 40 μM while maintaining the DA concentration constant (5 μM). The curve of I_{pa} vs concentration of PA is depicted in Fig. 14B and it is linear. The result confirms that changing the concentration of one analyte does not affect the peak current and peak potential of another analyte; it also demonstrates the modified carbon paste electrode's outstanding selectivity and sensitivity towards DA and PA.

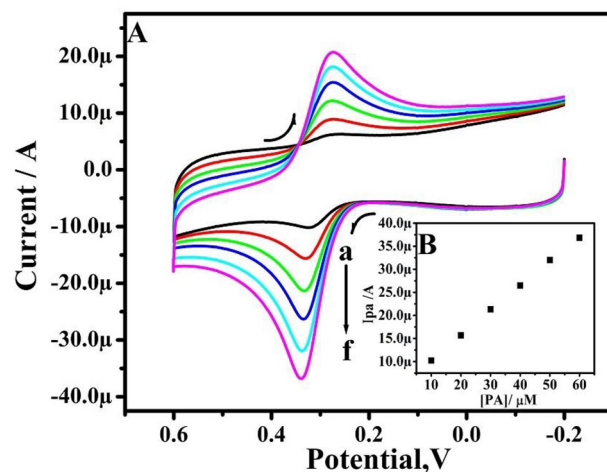


Figure 10. (A) CVs of 10 μM PA in 0.2 M PBS solution of pH 7.4 at TX-100-PT-MCPE at a sweep rate of 50 mV/s with different concentrations (a–f: 10–60 μM). (B) Graph of anodic peak current versus concentration of PA.

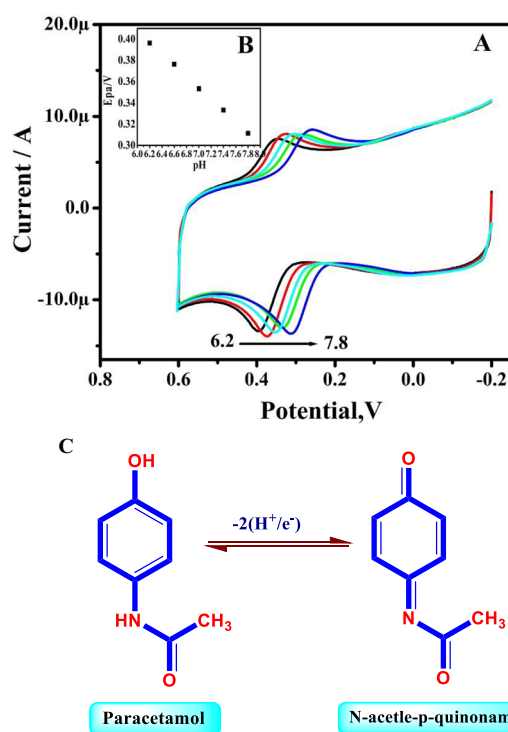


Figure 11. (A) Cyclic voltammograms of 10 μM PA for different pH (from a–e; 6.2–7.8 pH) at pretreated TX-100 modified CPE. (B) Graph of E_{pa} versus different pH. (C) Redox mechanism paracetamol.

Real sample analysis. For the examination of DA-containing injectable samples and PA tablet samples by standard addition method using TX-100PT-MCPE. The injection samples and DA injection were utilized after a sufficient dilution with a 0.2 M phosphate buffer. Dolo-500, Micro Labs Ltd provided the PA tablet sample, which had a PA 500 mg concentration. The obtained results are tabulated in Table 4. The recovery was accept-

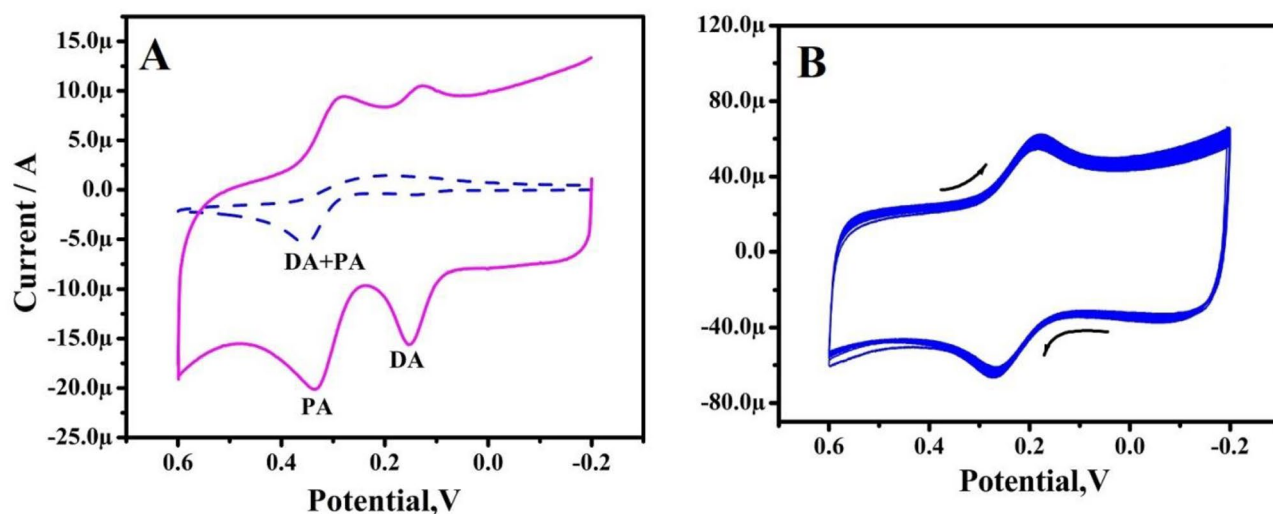


Figure 12. (A) CVs for simultaneous determination for 10 μM DA and 10 μM PA at BCPE (dashed line) and TX-100-PT-MCPE (solid line) at a sweep rate of 100 mV/s. (B) CVs of 1 mM potassium ferrocyanide in 1 M KCl solution at a speed rate of 50 mV/s for stability analysis for TX-100-PT-MCPE at 50 cycles.

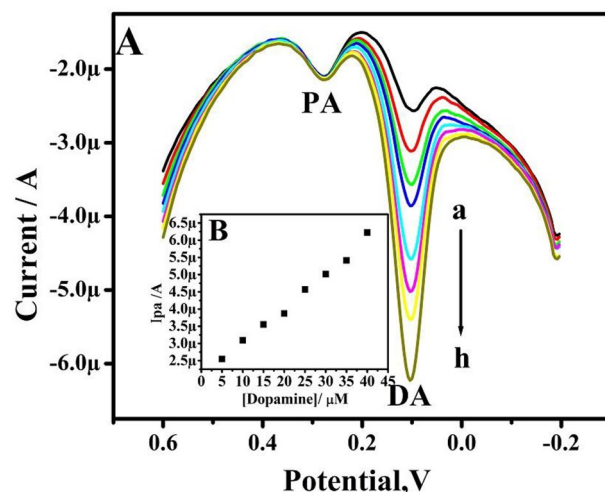


Figure 13. (A) Differential pulse voltammograms were obtained for variation of concentration 5–40 μM (a–h) DA, in PBS (pH 7.4), in the presence of 5 μM PA at TX-100-PT-MCPE. (B) Graph of anodic peak current versus concentration of DA.

able, indicating that the proposed methods may be utilized to detect DA in injections with a recovery rate of 98.20–99.10 percent and a recovery rate of 98.5–99.45 percent for the PA tablet sample.

Conclusion

The pretreatment of the CPE with TX-100 in 0.1 M NaOH solution results in a very stable DA sensor with outstanding sensitivity and selectivity. The TX-100PT-MCPE reduced the overpotential and enhanced the current responsiveness. The pH study reveals that the redox mechanism involves an equal quantity of protons and electrons being transferred. This demonstrated a promising biological use. The prepared electrode showed satisfactory stability when kept under ambient conditions. The proposed approach is also used to identify DA in injectable samples and PA in commercial tablet formulations.

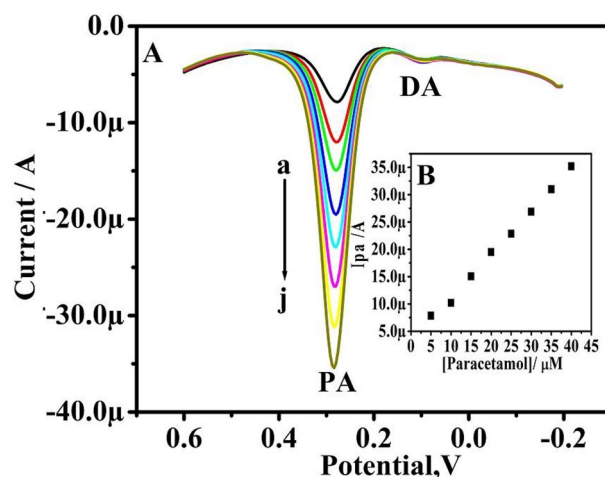


Figure 14. (A) Differential pulse voltammograms obtained for variation of concentration 5–40 μM (a–h) PA, in PBS (pH 7.4), in the presence of 5 μM DA at pretreated TX-100 modified CPE. (B) Graph of anodic peak current versus concentration of PA.

Sample	DA added (μM)	Found (μM)	Recovery (%)
DA injections	10	9.84	98.4 \pm 0.976
	20	19.46	98.20 \pm 0.876
	30	29.73	99.10 \pm 0.135
PA tablet	10	9.85	98.5 \pm 0.911
	20	19.69	98.45 \pm 0.992
	30	29.28	97.6 \pm 0.997

Table 4. Detection of DA and PA in the real sample (n = 3).

Received: 10 November 2021; Accepted: 15 November 2022

Published online: 24 November 2022

References

- Abdel Rahim, A. M. & Abdel Gaber, A. A. Fabrication and characterization of extrinsic electrochemically modified graphite reinforcement carbon paste electrode for selective determination of Cu(II) in trace levels. *Appl. Surf. Sci. Adv.* **2**, 100031 (2020).
- Cariati, L. S. S. & Buoro, R. M. Evaluation of ionic natural deep eutectic solvents (NADES) modified binders towards the chemical properties of carbon paste electrodes. *Electrochem. Commun.* **109**, 106605 (2019).
- Walid, B. *et al.* Elaboration of carbon paste electrode containing pentadentate Nickel-(II) Schiff base complex: Application to electrochemical oxidation of thiosulfate in alkaline medium. *Arab. J. Chem.* **13**(7), 6072–6083 (2020).
- Olga, V. *et al.* Use of carbon paste electrode and modified by gold nanoparticles for selected macrolide antibiotics determination as standard and in pharmaceutical preparations. *J. Electroanal. Chem.* **873**, 114324 (2020).
- Mehdi, R.-N. *et al.* A modified sensitive carbon paste electrode for 5-fluorouracil based using a composite of praseodymium erbium tungstate. *Microchem. J.* **154**, 104654 (2020).
- Piovesan, J. V., Santana, E. R. & Almir, S. A carbon paste electrode improved with poly (ethylene glycol) for tannic acid surveillance in beer samples. *Food Chem.* **326**, 127055 (2020).
- Saleh, A. T., Khaled, M. M. & Abdur, R. Electrochemical sensor for the determination of ketoconazole based on gold nanoparticles modified carbon paste electrode. *J. Mol. Liq.* **256**, 39–48 (2018).
- Janata, J. & Josowicz, M. Conducting polymers in electronic chemical sensors. *Nat. Mater.* **2**, 19–24 (2003).
- Cristina, S. *et al.* Sensitive voltammetry determination of riboflavin in pharmaceutical and biological samples using FSN-Zonyl-Nafion modified carbon paste electrode. *Microchem. J.* **155**, 104729 (2020).
- Lili, Z., Yuhua, C. & Guangqun, C. Electrochemical sensor based on magnetic molecularly imprinted nanoparticles at surfactant modified magnetic electrode for determination of bisphenol A. *Biosens. Bioelectron.* **54**, 258–261 (2014).
- Thomas, T. *et al.* Pristine multi-walled carbon nanotubes/SDS modified carbon paste electrode as an amperometric sensor for epinephrine. *Talanta* **125**, 352–360 (2014).
- Lokhande, P. E., Pawar, K. & Chavan, U. S. Chemically deposited ultrathin $\alpha\text{-Ni(OH)}_2$ nanosheet using surfactant on Ni foam for high-performance supercapacitor application. *Mater. Sci. Energy Technol.* **1**, 166–170 (2018).
- Biaselle, C. J. & Millar, D. B. Studies on triton X-100 detergent micelles. *Biophys. Chem.* **3**, 355 (1975).
- Jayaprakash, G. K. & Flores-Moreno, R. Quantum chemical study of TX-100 modified graphene surface. *Electrochim. Acta* **248**, 225–231 (2017).
- Marzieh, M. & Shahla, E. Colorimetric detection of insulin in human serum using GO/AuNPs/TX-100 nanocomposite. *Spectrochim. Acta Part A Mol. Biomol. Spectrosc.* **240**, 118617 (2020).
- Jayaprakash, G. K., Kumara Swamy, B. E., Casillas, N. & Flores-Moreno, R. Analytical Fukui and cyclic voltammetric studies on ferrocene modified carbon electrodes and effect of TX-100 on it. *Electrochim. Acta* **258**, 1025–1034 (2017).

17. Chandrashekhara, B. N. & Kumara Swamy, B. E. Simultaneous cyclic voltammetric determination of norepinephrine, ascorbic acid and uric acid using TX-100 modified carbon paste electrode: A cyclic voltammetric study. *Anal. Methods* **4**, 849 (2012).
18. Fang, J., Xie, Z., Wallace, G. & Wang, X. Co-deposition of carbon dots and reduced graphene oxide nanosheets on carbon-fiber microelectrode surface for selective detection of dopamine. *Appl. Surf. Sci.* **412**, 131–137 (2017).
19. Andrea, P., Rojas, S., Cortes, M. & Hurtado, J. Electrochemical synthesis of poly (3,4-ethylene dioxithiophene) doped with a new bis(pyrazolyl)methane disulfonate and its behaviour towards dopamine detection. *J. Electroanal. Chem.* **837**, 200–207 (2019).
20. Rana, A., Baig, N. & Saleh, T. A. Electrochemically pretreated carbon electrodes and their electroanalytical applications—a review. *J. Electroanal. Chem.* **833**, 313–332 (2019).
21. Sukanya Swamy, B. E. K., Shashikumara, J. K., Sharma, S. C. & Hariprasad, S. A. Poly (Orange CD) sensor for paracetamol in presence of folic acid and dopamine. *Sci. Rep.* **11**, 22332 (2021).
22. Flores-Moreno, R., Urbina, K. P. & Sandoval, Z. G. Sinapsis, Version XII-V. Sinapsis developers, 2012. (Version: Sinapsis. XIII Weblink: <http://sinapsis.sourceforge.net>. Accessed 20 July 2020).
23. Gerald, G. *et al.* demon2k. *Wiley Interdiscip. Rev. Comput. Mol. Sci.* **2**, 548–555 (2012).
24. Perdew, J. P. *et al.* Generalized gradient approximation made simple. *Phys. Rev. Lett.* **77**, 3865–3868 (1996).
25. Perdew, J. P. *et al.* Generalized gradient approximation made simple. *Phys. Rev. Lett.* **78**, 1396–1396 (1997).
26. Godbout, N. *et al.* Optimization of Gaussian-type basis sets for local spin density functional calculations. Part I. Boron through neon, optimization technique and validation. *Can. J. Chem.* **70**, 560–571 (1992).
27. Parr, R. G. & Yang, W. Density functional approach to the frontier–electron theory of chemical reactivity. *J. Am. Chem. Soc.* **106**, 4049–4050 (1984).
28. Jayaprakash, G. K. *et al.* Dual descriptor analysis of cetylpyridinium modified carbon paste electrodes for ascorbic acid sensing applications. *J. Mol. Liquids* **334**, 116348/1–17 (2021).
29. Jayaprakash, G. K. *et al.* Electrochemical and quantum chemical studies of cetylpyridinium bromide modified carbon electrode interface for sensor applications. *J. Mol. Liq.* **315**(113719), 1–10 (2020).
30. Shashikumara, J. K. *et al.* Effect of RGO-Y₂O₃ and RGO-Y₂O₃:Cr³⁺ nanocomposite sensor for dopamine. *Sci. Rep.* **11**, 9372/1–11 (2021).
31. Pruneanu, S. *et al.* The influence of uric and ascorbic acid on the electrochemical detection of dopamine using graphene-modified electrodes. *Electrochim. Acta* **154**, 197 (2015).
32. Thiagarajan, S. & Chen, S. M. Preparation and characterization of Pt Au hybrid film modified electrodes and their use in the simultaneous determination of dopamine, ascorbic acid and uric acid. *Talanta* **74**(2), 212–222 (2007).
33. Corona-Avendano, S. *et al.* Influence of CTAB on the electrochemical behaviour of dopamine and its analytic determination in the presence of ascorbic acid. *J. Appl. Electrochem.* **40**, 463 (2010).
34. Ali Kamyabi, M. & Aghajanloo, F. Electrocatalytic response of dopamine at a CPE modified with ferrocene. *Roat Che Act* **82**, 599–606 (2009).
35. Sunil Kumar Naik, T. S., Muthui Martin, M. & Kumara Swamy, B. E. Fabrication of poly (Sudan III) modified carbon paste electrode sensor for dopamine: A voltammetric study. *J. Electroanal. Chem.* **834**, 73 (2018).
36. Goyal, R. N. & Singh, S. P. Simultaneous voltammetric determination of dopamine and adenosine using a single-walled carbon nanotube—MCPE. *Carbon* **46**, 1556–1562 (2008).
37. Wang, Q., Li, N. & Wang, W. Electrocatalytic response of dopamine at a metallothioneins self-assembled gold electrode. *Anal. Sci.* **18**, 635 (2002).
38. Zhu, Z. *et al.* Electrochemical detection of dopamine on a Ni/Al layered double hydroxide modified carbon ionic liquid electrode. *Sens. Actuators B* **151**, 146–152 (2010).
39. Kaur, B., Pandiyan, T., Satpati, B. & Srivastava, R. Simultaneous and sensitive determination of ascorbic acid, dopamine, uric acid, and tryptophan with silver nanoparticles-decorated reduced graphene oxide modified electrode. *Colloids Surf. B* **111**, 97–106 (2013).
40. Silva, L. V. D. *et al.* Amperometric sensor based on carbon nanotubes and electropolymerized vanillic acid for simultaneous determination of ascorbic acid, dopamine, and uric acid. *J. Solid State Electrochem.* **20**, 2389–2393 (2016).
41. Chih, Y. K. & Yang, M. C. Simultaneous detection of dopamine and ascorbic acid using silver. *Taiwan Inst. Chem. Eng.* **45**, 833–839 (2014).
42. Liu, R. *et al.* A glassy carbon electrode modified with an amphiphilic, electroactive and photosensitive polymer and with multi-walled carbon nanotubes for simultaneous determination of dopamine and paracetamol. *Microchim. Acta* **183**, 1543–1551 (2016).
43. Shashikumara, J. K., KumaraSwamy, B. E. & Madhuchandra, H. D. Poly (amido black) modified carbon paste electrode sensor for dopamine in the presence of uric acid. *Mater. Sci. Energy Technol.* **3**, 390–396 (2020).
44. Yang, Y. J. & Li, W. K. CTAB functionalized graphene oxide/multiwalled carbon nanotube composite modified electrode for the simultaneous determination of ascorbic acid, dopamine, uric acid and nitrite. *Sens. Actuators B Chem.* **56**, 300–306 (2014).
45. de Matos Morawski, F. *et al.* A novel electrochemical platform based on mesoporous silica/titania and gold nanoparticles for simultaneous determination of norepinephrine and dopamine. *Mater. Sci. Eng. C* **120**, 111646 (2021).
46. Roduan, M. R. A. M. *et al.* New modified mesoporous silica nanoparticles with bimetallic Ni-Zr for electroanalytical detection of dopamine. *J. Electrochem. Sci. Eng.* **12**, 463–474 (2022).
47. Ahmed, J., Faisal, M., Harraz, F. A., Jalalah, M. & Alsareii, S. A. Development of an amperometric biosensor for dopamine using novel mesoporous silicon nanoparticles fabricated via a facile stain etching approach. *Phys. E* **135**, 114952 (2022).

Author contributions

J.K.S.K.: electrochemical sensors experiments, formal analysis, writing—original draft. B.E.K.S.: conceptualization, supervision, writing—review and editing. G.K.J.: theoretical work, writing—review. S.C.S.: writing—review and editing. R.F.-M.: theoretical work, writing—review. K.M.: writing—review. S.A.H.: writing—review and editing.

Funding

This article was funded by Jain University.

Competing interests

The authors declare no competing interests.

Additional information

Correspondence and requests for materials should be addressed to B.E.K.S. or S.C.S.

Reprints and permissions information is available at www.nature.com/reprints.

Publisher's note Springer Nature remains neutral with regard to jurisdictional claims in published maps and institutional affiliations.



Open Access This article is licensed under a Creative Commons Attribution 4.0 International License, which permits use, sharing, adaptation, distribution and reproduction in any medium or format, as long as you give appropriate credit to the original author(s) and the source, provide a link to the Creative Commons licence, and indicate if changes were made. The images or other third party material in this article are included in the article's Creative Commons licence, unless indicated otherwise in a credit line to the material. If material is not included in the article's Creative Commons licence and your intended use is not permitted by statutory regulation or exceeds the permitted use, you will need to obtain permission directly from the copyright holder. To view a copy of this licence, visit <http://creativecommons.org/licenses/by/4.0/>.

© The Author(s) 2022